Low-Voltage Junctionless Oxide-Based Thin-Film Transistors Self-Assembled by a Gradient Shadow Mask

Guodong Wu, Jumei Zhou, Hongliang Zhang, Liqiang Zhu, and Qing Wan

***Abstract*—A gradient shadow-mask diffraction method is proposed for the fabrication of junctionless indium–tin–oxide (ITO) and indium–zinc–oxide (IZO) thin-film transistors (TFTs) with different channel thicknesses on one glass substrate during one-batch radio-frequency magnetron sputtering. The operation mode and saturation field-effect mobility of the room-temperature-processed oxide-based junctionless TFTs are channel thickness dependent, and the threshold voltages shift from negative to positive when the self-assembled channel thickness is reduced to a critical thickness.**

***Index Terms*—Gradient mask diffraction, junctionless thin-film transistors (TFTs), operation mode modulation.**

I. INTRODUCTION

OXIDE-based thin-film transistors (TFTs) have attracted much attention for potential applications in flat-panel displays, sensors, and radio-frequency (RF) identification [1], [2]. Modulation of the threshold voltage and operation mode of oxide-based TFTs is of particularly high importance for realization of integrated circuits and relevant applications in chemical and biological sensors [3], [4]. Up to now, there are several methods to tune the threshold voltage and operation mode, such as chemical doping [5], tuning the oxygen concentration during channel deposition [6], an additional channel layer deposition [7], etc. Among these methods, changing the thickness of an active channel layer is the most effective approach [8], [9]. However, a multibatch process was still needed to change the channel thickness to tune the threshold voltage and operation mode. Up to now, a simplified one-batch process is still a big challenge for low-cost applications.

In this letter, low-voltage indium–tin–oxide (ITO)-based and indium–zinc–oxide (IZO)-based TFTs with different channel thicknesses were self-assembled on one ITO glass substrate by one-batch sputtering deposition with a gradient shadow mask. A junctionless device structure was obtained because the source/drain electrodes and the self-assembled channel layer have the same chemical composition. Depletion-mode to enhancement-mode conversion can be realized when the self-assembled channel thickness is reduced to a critical thickness, although the resistivity of ITO and IZO films is as low as $1.2 \times 10^{-3}\ \Omega \cdot \mathrm{cm}$.

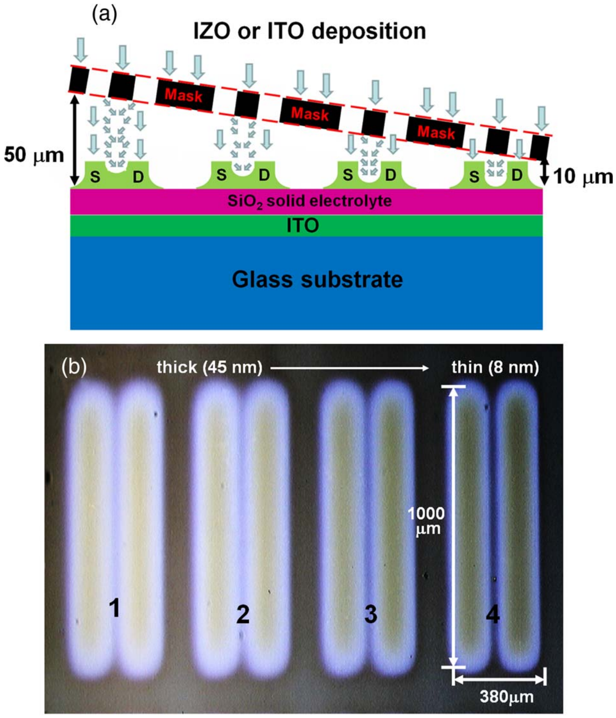

Fig. 1. (a) Schematic of junctionless oxide-based TFTs with different channel thicknesses fabricated by a gradient mask method. (b) Optical image of the four self-assembled junctionless IZO-based TFTs with different channel thicknesses.

II. EXPERIMENTAL DETAILS

Junctionless ITO- and IZO-based TFTs were self-assembled on conductive ITO glass substrates by a fully room-temperature process. Fig. 1(a) and (b) shows the schematic and optical image of four junctionless TFTs with different channel thicknesses on one glass substrate by one-batch sputtering deposition with a gradient nickel shadow mask, respectively. First, 1.5-μm-thick SiO_2 electrolyte films were deposited onto ITO glass substrates by plasma-enhanced chemical vapor deposition using SiH_4 and O_2 as reactive gases at room temperature.

Manuscript received August 19, 2012; revised September 2, 2012; accepted September 2, 2012. Date of publication October 18, 2012; date of current version November 22, 2012. This work was supported in part by the National Program on Key Basic Research Project under Grant 2012CB933004, by the National Natural Science Foundation of China under Grant 11174300, and by the Fok Ying Tung Education Foundation under Grant 121063. The review of this letter was arranged by Editor A. Chin.

The authors are with Ningbo Institute of Materials Technology and Engineering, Chinese Academy of Sciences, Ningbo 315201, China (e-mail: wanqing@nimte.ac.cn).

Color versions of one or more of the figures in this letter are available online at http://ieeexplore.ieee.org.

Digital Object Identifier 10.1109/LED.2012.2217934

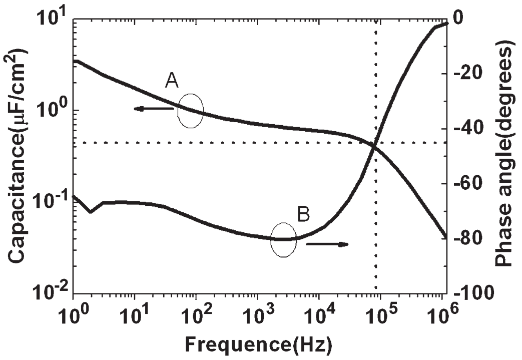

Fig. 2. (Curve A) Frequency-dependent specific capacitance and (curve B) phase angle of the room-temperature-deposited SiO_2-based solid electrolyte film.

The flow rate ratio of SiH_4 and O_2 was 3.0 sccm/18 sccm. The deposition pressure and deposition time were 30 Pa and 20 min, respectively. Then, 150-nm ITO or IZO source/drain electrodes were deposited on the SiO_2 electrolyte films by RF magnetron sputtering in pure Ar ambient with a gradient nickel shadow mask. Thin ITO or IZO channels will be self-assembled between the source and drain electrodes during sputtering due to the diffraction effect. The distance between the nickel mask and the substrate for the gradient shadow mask is designed to be 50 μm for the far edge and ~10 μm for the near edge. Hence, during one-batch deposition, self-aligned TFTs with different active channel thicknesses can be simultaneously fabricated. The frequency-dependent capacitance and phase angle of the SiO_2-based electrolyte films were measured by a Solartron 1260 impedance analyzer. The electrical characteristics of the self-assembled junctionless devices with different ITO or IZO channel thicknesses were measured by a Keithley 4200 semiconductor parameter analyzer at room temperature in the dark. Here, we should point out that metal probes are connected to the ITO or IZO source/drain regions directly for electrical performance measurement.

III. RESULTS AND DISCUSSION

Fig. 2 shows the frequency-dependent specific capacitance and phase angle of the SiO_2 electrolyte film in the frequency range from 1.0 Hz to 1.0 MHz. The specific capacitance increases with decreasing frequency, and a value of ~3.5 μF/cm^2 at 1.0 Hz is measured. The main contribution to the capacitance at low frequency is due to the electric-double-layer (EDL) effect at the SiO_2 electrolyte/electrode interfaces [10]. The large specific capacitance provides a strong electrostatic couple between the gate electrode and the self-assembled ITO and IZO active channels, which is favorable for realizing low-voltage operation. As shown by curve B in Fig. 2, the phase angle is less than -45° when the frequency is lower than 80 kHz, which is favorable for EDL formation. However, at a higher frequency $(f > 80$ kHz), the ion mobility limits the response time, and only few ions in the SiO_2 electrolyte can accumulate at the interface. Thus, ionic relaxation is the dominating polarization mechanism at high frequency.

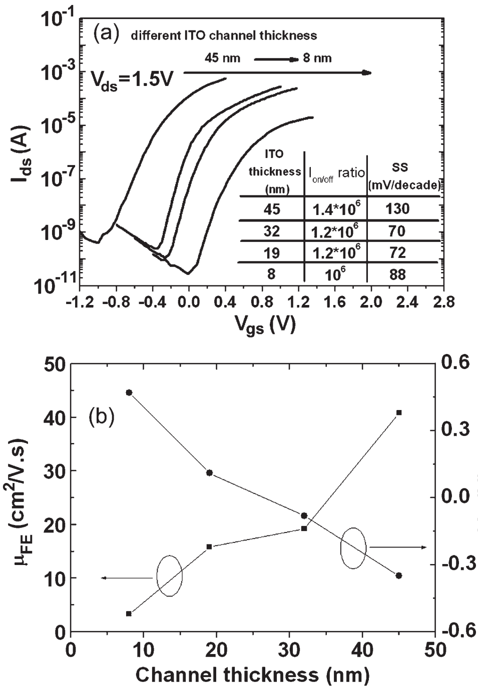

Fig. 3. (a) Transfer characteristics of ITO-based TFTs with different ITO channel layer thicknesses ($V_{ds} = 1.5$ V). (b) Variations of $V_{\rm th}$ and $\mu_{\rm FE}$ of the junctionless ITO-based TFTs as a function of the channel thickness.

Fig. 3(a) shows the transfer curves of the self-assembled junctionless TFTs with ITO channel thickness change from 45 to 8 nm at a drain-to-source voltage $V_{ds} = 1.5$ V. The transfer curve shifts from negative to positive when the channel thickness is reduced. All devices show a small subthreshold swing (SS) of less than 130 mV/dec and a drain current on/off ratio of $\sim 10^6$. The saturation field-effect mobility $\mu_{\rm FE}$ is calculated from the following equation: $I_{DS} = (C_i \mu W/2L)(V_{GS} - V_{\rm th})^2$, where $L = 80$ μm is the channel length, and $W = 1000$ μm is the channel width. C_i is the specific capacitance of the SiO_2 electrolyte gate dielectric (3.5 μF/cm^2 at 1.0 Hz). Fig. 3(b) shows the channel-thickness-dependent saturation field-effect mobility $\mu_{\rm FE}$ and threshold voltage $V_{\rm th}$ of the ITO-based junctionless devices. $\mu_{\rm FE}$ decreases from 40.8 to 3.3 $\rm cm^2/V \cdot s$ and $V_{\rm th}$ shifts from -0.35 to 0.47 V when the self-assembled ITO channel thickness is reduced from 45 to 8 nm.

Fig. 4(a) shows the transfer curves of the IZO-based junctionless TFTs with different channel thicknesses at $V_{ds} = 1.5$ V. All TFTs show a small SS of $<$ 130 mV/dec. The channel-thickness-dependent saturation field-effect mobility and threshold voltage are shown in Fig. 4(b). $\mu_{\rm FE}$ reduces from 30.6 to 7.2 $\rm cm^2/V \cdot s$ when the IZO channel thickness is reduced from ~45 to ~8 nm. Depletion-mode $(V_{\rm th} = -0.3$ V) to enhancement-mode $(V_{\rm th} = 0.34$ V) conversion is observed when the IZO channel thickness is reduced from 45 to 8 nm. Similar channel-thickness-dependent electrical properties were also observed for normal In_2O_3-based TFTs [11]. SS reduces with channel thickness reduction first, but slight degradation was observed when the channel thickness is reduced to 8 nm due to the surface scattering and absorption effect.

The positive shift of $V_{\rm th}$ is due to the reduction of the absolute carrier number in the self-assembled ITO and IZO channels [11]. At the same time, the channel layers are directly

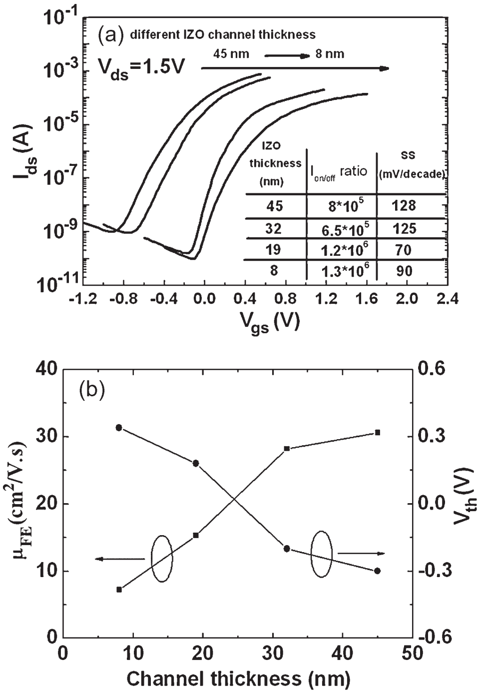

IZO thickness (nm)	$I_{on/off}$ ratio	SS (mV/decade)
45	8*10^5	128
32	6.5*10^5	125
19	1.2*10^6	70
8	1.3*10^6	90

Fig. 4. (a) Transfer characteristics of IZO-based TFTs with different IZO channel layer thicknesses ($V_{ds} = 1.5$ V). (b) Variations of V_{th} and μ_{FE} of the junctionless IZO-based TFTs as a function of the channel thickness.

exposed to air ambient, which results in oxygen adsorption on the channel surface [12]. Therefore, the adsorbed oxygen can capture electrons from the conduction band and result in channel surface depletion. If the oxide-based channel thickness is thin enough, enhancement-mode operation is possible, although ITO and IZO are highly conductive. Hall effect measurement results indicate that the resistivity of IZO films with four thicknesses shows a resistivity of $\sim 1.2 \times 10^{-3}\ \Omega \cdot \mathrm{cm}$. When the thickness of the IZO film reduces from 45 to 8 nm, the carrier concentration linearly decreases from $1.72 \times 10^{20}/\mathrm{cm}^3$ to $1.63 \times 10^{20}/\mathrm{cm}^3$, respectively. Here, lower field-effect mobility was measured for devices with thinner ITO or IZO active layers. Oxide-based TFTs were self-assembled on ITO glass substrates with relatively large surface roughness and measured in air ambient without surface passivation; hence, interfacial scattering and water or oxygen absorption are more serious for thinner channels. In fact, Dhananjay *et al.* found that the field-effect mobility of In_2O_3 TFTs was clearly channel thickness dependent and that it reduced from 14 $\mathrm{cm}^2/\mathrm{V} \cdot \mathrm{s}$ for a 20-nm channel to less than 0.01 $\mathrm{cm}^2/\mathrm{V} \cdot \mathrm{s}$ for a 5-nm channel [9]. Our results are in good agreement with their reported results.

In addition, we should point out that only the channel area very close to the source/drain electrodes has a serious diffraction effect during RF sputtering and that other channel areas have a relatively uniform thickness. At the same time, our experiment results demonstrated that IZO and ITO films with thickness up to 60 nm can be tuned off by SiO_2 electrolytes due to the strong EDL capacitance. Hence, only slight overestimation of field-effect mobility would be exhibited for the self-assembled TFTs with thickest channel of 45 nm [10].

IV. CONCLUSION

In summary, a novel method based on a gradient shadow mask has been proposed for junctionless low-voltage oxide-based TFTs with different channel thicknesses fabricated during one-batch sputtering. The operation mode can be modulated from depletion mode to enhancement mode for both ITO- and IZO-based TFTs.

REFERENCES

[1] R. L. Hoffman, B. J. Norris, and J. F. Wager, “ZnO-based transparent thin-film transistors,” *Appl. Phys. Lett.*, vol. 82, no. 5, pp. 733–735, Feb. 2003.
[2] K. Nomura, H. Ohta, K. Ueda, T. Kamiya, M. Hirano, and H. Hosono, “Thin-film transistor fabricated in single-crystalline transparent oxide semiconductor,” *Science*, vol. 300, no. 5623, pp. 1269–1272, May 2003.
[3] H. S. Lee, C. H. Park, K. H. Lee, D. H. Kim, H. R. Kim, G. H. Lee, and S. Im, “Threshold voltage control by gate electrode in Ga–Sn–Zn–O thin-film transistors for logic inverter application,” *Phys. Stat. Sol.-Rapid Res. Lett.*, vol. 5, no. 5/6, pp. 211–213, Jun. 2011.
[4] Z. X. Shi and D. Z. Zhu, “Research of CMOS biosensor IC for extra-cellular electrophysiological signal recording and pH value measuring,” *J. Semicond.*, vol. 30, no. 9, pp. 71–76, Sep. 2009.
[5] P. Pacher, A. Lex, V. Proschek, H. Etschmaier, E. Tchernychova, M. Sezen, U. Scherf, W. Grogger, G. Trimmel, C. Slugovc, and E. Zojer, “Chemical control of local doping in organic thin-film transistors: From depletion to enhancement,” *Adv. Mater.*, vol. 20, no. 16, pp. 3143–3148, Aug. 2008.
[6] J. Sun, J. Jiang, A. Lu, and Q. Wan, “One-volt oxide thin-film transistors on paper substrates gated by SiO_2-based solid electrolyte with controllable operation modes,” *IEEE Trans. Electron Devices*, vol. 57, no. 9, pp. 2258–2263, Sep. 2010.
[7] Y. Abe, T. Hasegawa, Y. Takahashi, T. Yamada, and Y. Tokura, “Control of threshold voltage in pentacene thin-film transistors using carrier doping at the charge–transfer interface with organic acceptors,” *Appl. Phys. Lett.*, vol. 87, no. 15, pp. 153506-1–153506-3, Oct. 2005.
[8] J. S. Park, J. K. Jeong, Y. G. Mo, H. D. Kim, and C. J. Kim, “Control of threshold voltage in ZnO-based oxide thin film transistors,” *Appl. Phys. Lett.*, vol. 93, no. 3, pp. 033513-1–033513-3, Jul. 2008.
[9] K. Dhananjay, S.-S. Cheng, C.-Y. Yang, C.-W. Ou, Y.-C. Chuang, M. C. Wu, and C.-W. Chu, “Dependence of channel thickness on the performance of In_2O_3 thin-film transistors,” *J. Phys.D, Appl. Phys.*, vol. 41, no. 9, pp. 092006-1–092006-6, May 2008.
[10] A. Lu, J. Sun, J. Jiang, and Q. Wan, “One-shadow-mask self-assembled ultralow-voltage coplanar homojunction thin-film transistors,” *IEEE Electron Device Lett.*, vol. 31, no. 10, pp. 1137–1139, Oct. 2010.
[11] J. H. Noh, S. Y. Ryu, S. J. Jo, C. S. Kim, S.-W. Sohn, P. D. Rack, D.-J. Kim, and H. K. Baik, “Indium oxide thin-film transistors fabricated by RF sputtering at room temperature,” *IEEE Electron Device Lett.*, vol. 31, no. 6, pp. 567–569, Jun. 2010.
[12] J. S. Park, J. K. Jeong, H. J. Chung, H. D. Kim, and C. J. Kim, “Electronic transport properties of amorphous indium–gallium–zinc oxide semiconductor upon exposure to water,” *Appl. Phys. Lett.*, vol. 92, no. 7, pp. 072104-1–072104-3, Feb. 2008.